Journal of Materials Chemistry A

PAPER

View Article Online
View Journal | View Issue

Cite this: J. Mater. Chem. A, 2016, 4, 17726

Thermal stability of $Mg_2Si_{0.4}Sn_{0.6}$ in inert gases and atomic-layer-deposited Al_2O_3 thin film as a protective coating

Libin Zhang,*[a] Xi Chen,[a] Yinglu Tang,[b] Li Shi,[ac] G. Jeffrey Snyder,[bd] John B. Goodenough[ac] and Jianshi Zhou[ac]

Received 2nd September 2016
Accepted 20th October 2016

DOI: 10.1039/c6ta07611d

www.rsc.org/MaterialsA

$Mg_2Si_{1-x}Sn_x$ solid solutions are promising thermoelectric materials to be applied in vehicle waste-heat recovery. Their thermal stability issue, however, needs to be addressed before the materials can be applied in practical thermoelectric devices. In this work, we studied the crystal structure and chemical composition of $Mg_2Si_{1-x}Sn_x$ in inert gas atmosphere up to 823 K. We found that the sample was oxidized even in high-purity inert gases. Although no obvious structural change has been found in the slightly oxidized sample, carrier concentration decreased significantly since oxidation creates Mg vacancies in the lattice. We demonstrated that an atomic-layer deposited Al_2O_3 coating can effectively protect $Mg_2Si_{1-x}Sn_x$ from oxidation in inert gases and even in air. In addition, this Al_2O_3 thin film also provides *in situ* protection to the Sb-doped $Mg_2Si_{1-x}Sn_x$ samples during the laser-flash measurement and therefore eliminates the measurement error that occurs in uncoated samples as a result of sample oxidation and graphite exfoliation issues.

I. Introduction

Thermoelectric materials have attracted vast research interests for their applications in waste-heat recovery and refrigeration.[1] $Mg_2Si_{1-x}Sn_x$ solid solutions are among the most promising n-type thermoelectric materials for vehicle waste-heat recovery owing to their high thermoelectric performance as well as light weight, low cost, earth abundance, and environmental friendliness of the major constituent elements.[2] A dimensionless figure-of-merit (ZT) is commonly used to evaluate the thermoelectric performance of a material:

$$ZT = \frac{S^2\sigma}{\kappa}T \quad (1)$$

where S is the Seebeck coefficient, σ is the electrical conductivity, $S^2\sigma$ is the power factor, κ is the thermal conductivity, and T is the absolute temperature. Due to a peculiar band-converging feature in the conduction-band edge, $Mg_2Si_{1-x}Sn_x$ ($x = 0.6$–0.7) solid solutions with optimized electron doping can achieve a high thermoelectric power factor.[2–4] Moreover, the lattice thermal conductivity of $Mg_2Si_{1-x}Sn_x$ is also effectively reduced by the alloying effect in the solid solution.[2–4] Therefore, an optimized electron doping in $Mg_2Si_{1-x}Sn_x$ ($x = 0.6$–0.7) solid solutions leads to a $ZT = 1.1$–1.3.[2–5] However, the thermal stability issue of $Mg_2Si_xSn_x$ solid solution is a major obstacle that must be tackled before the material can be applied in practical thermoelectric devices.[6–10]

Tani *et al.* found that Mg_2Si starts to react with air significantly above 723 K and the oxidation layer develops into the sample by oxygen diffusion.[6] Bourgeois *et al.* studied the thermal stability of $Mg_2Si_{1-x}Sn_x$ solid solutions by *in situ* temperature X-ray powder diffraction in Ar gas. They found $Mg_2Si_{1-x}Sn_x$ powders begin to decompose into MgO, Si and Sn at 630 K; the dense pellets decompose at a much slower rate than the powder sample owing to their smaller specific surface area.[7] Søndergaard *et al.* found that in both $Mg_2Si_{0.4}Sn_{0.6}$ and $Mg_2Si_{0.6}Sn_{0.4}$, a Sn-rich $Mg_2Si_{1-x}Sn_x$ phase segregates quickly upon heating to 673 K in air.[8] Skomedal *et al.* pointed out that in $Mg_2Si_{1-x}Sn_x$ compounds, Sn-rich solid solutions decompose faster at lower temperatures compared to the Si-rich solid solutions.[9] Yin *et al.* examined the thermal stability of $Mg_2Si_{0.3}Sn_{0.7}$ in vacuum as well as in air. When heated at 773 K in vacuum, the $Mg_2Si_{0.3}Sn_{0.7}$ solid solution suffers a severe Mg loss due to the high vapor pressure of Mg; when heated in air without protection, the sample was oxidized.[10]

Besides the chemical instability, the influences of heat treatment on transport properties in $Mg_2Si_{1-x}Sn_x$ have also been examined. Bourgeois *et al.* found that in unprotected intrinsic $Mg_2Si_{1-x}Sn_x$ solid solutions, both the electrical resistivity and thermoelectric power curves are repeatable when the

[a]Materials Science and Engineering Program, The University of Texas at Austin, Austin, Texas 78712, USA. E-mail: libinzhang@utexas.edu
[b]Department of Materials Science, California Institute of Technology, Pasadena, California 91125, USA
[c]Department of Mechanical Engineering, The University of Texas at Austin, Austin, Texas 78712, USA
[d]Department of Materials Science and Engineering, Northwestern University, Evanston, Illinois 60208, USA

temperature cycles up to 770 K.[7] However, Yin *et al.* found that after a heat treatment at 823 K, the BN-coated $Mg_2(Si_{0.3}Sn_{0.7})_{0.98}Sb_{0.02}$ exhibits reduced carrier concentration and carrier mobility owing to the Mg loss and Sn precipitation during the heat treatment.[10] As discussed in Section IIIB of this paper, these two observations do not contradict each other.

To avoid the thermal degradation in $Mg_2Si_{1-x}Sn_x$ solid solutions, protective coatings on these compounds must be applied. Tani *et al.* fabricated a 0.7 μm β-$FeSi_2$ film on Mg_2Si pellet by RF magnetron-sputtering deposition in order to protect Mg_2Si from oxidation at 873 K.[6] Skomedal *et al.* briefly reported a micron-sized Al_2O_3 coating that effectively protects the $Mg_2Si_{0.4}Sn_{0.6}$ bulk from degradation at 673 K. However, the detail of the Al_2O_3 coating was not revealed.[9] Yin *et al.* applied a BN coating on $Mg_2Si_{0.3}Sn_{0.7}$ by spraying a layer of 0.5 mm BN, which provides a good protection of the sample up to 773 K; however, the carrier density in the sample deteriorates at 823 K.[10]

Most thermal stability studies of $Mg_2Si_{1-x}Sn_x$ reviewed above were performed in air. In this work, we investigated the thermal stability of $Mg_2Si_{1-x}Sn_x$ in inert gas atmospheres, where physical properties were monitored during thermal cycles. We found that thermal degradation of $Mg_2Si_{1-x}Sn_x$ takes place slowly even in inert gases, which leads to a reduced electron density and electrical conductivity. Inspired by the surface passivation of Al metal, we employed a nanoscale Al_2O_3 coating deposited by atomic-layer deposition (ALD) on the surface of a $Mg_2Si_{1-x}Sn_x$ pellet. In recent years, an Al_2O_3 thin film has become a popular passivation material for silicon in the microelectronic and photovoltaic industries.[11,12] The ALD-grown Al_2O_3 is amorphous and thus is able to provide a dense and uniform coverage over the sample surface. The ALD deposition mechanism also ensures a good adhesion of the Al_2O_3 layer to the sample surface. We find that an Al_2O_3-coated $Mg_2Si_{1-x}Sn_x$ is stable in inert gases at 823 K for 12 hours while the unprotected sample completely decomposed into MgO, Si and Sn during the same heating condition. The thermoelectric properties of Al_2O_3-coated $Mg_2Si_{1-x}Sn_x$ are not compromised after a temperature cycle. In addition, the nano-scale Al_2O_3 coating layer provides *in situ* protection to the $Mg_2Si_{1-x}Sn_x$ samples during the laser-flash measurement, which effectively eliminates measurement errors resulting from sample oxidation and exfoliation of the required graphite coating.

II. Methods

The $Mg_2Si_{0.4}Sn_{0.6}$ samples were synthesized by using the solid-state reaction method and pelletized using spark plasma sintering (SPS).[13] The as-prepared pellets had over 98% of their theoretical density. The pellets were cut into proper sizes and polished with 30-micron sand papers before performing the Al_2O_3 coating and physical-property measurements. The Al_2O_3 thin film was coated at 150 °C for 200 cycles with the Cambridge NanoTech Savannah 100 ALD apparatus. The Al_2O_3 growth rate is ~0.91 Å per cycle for the 150 °C recipe. The thickness of Al_2O_3 thin film was around 18 nm.

The phase purity and the crystal structure of samples were characterized by X-ray diffraction (XRD) on a Phillip X'pert diffractometer with Cu Kα radiation. A scanning electron microscopic (SEM) investigation and energy-dispersive X-ray spectroscopy (EDX) analysis was conducted with an FEI Quanta 650 ESEM. The thermogravimetric analysis (TGA) was conducted with a Mettler Thermogravimetric Analyzer, Model TGA/DSC 1. The thermoelectric properties, including Seebeck coefficient, electrical conductivity and thermal conductivity, were measured simultaneously from 2 K to 400 K with a physical properties measurement system (PPMS, Quantum Design). The scanning Seebeck coefficient measurement was conducted by utilizing a cold scanning thermocouple tip on heated samples.[14] The thermal diffusivity was measured by using the laser flash method on a Netzsch LFA 457 apparatus.

III. Results & analysis

A. Crystal structure and morphology

In order to investigate the thermal stability of $Mg_2Si_{0.4}Sn_{0.6}$ dense pellets in air as well as in inert gases, we conducted thermogravimetric analysis (TGA) up to 873 K at a heating rate of 3 K min^{-1} with air or N_2 gas (O_2 or H_2O < 20 PPM) flowing at a rate of 50 ml min^{-1}. As shown in Fig. 1(a), the as-made pellet started to gain weight around 700 K in air, indicating the onset of the samples oxidation; the oxidation became more severe above 800 K, as is manifested by the abrupt weight gain. The pellet became porous and brittle after TGA measurement and the XRD pattern shown in Fig. 1(b) indicates that the pellet partially decomposed into Si, Sn and MgO. For the as-made pellet heated in N_2 gas, the TGA curve indicates that the oxidation still took place beyond 700 K but was less severe compared to the sample studied in air. In fact, the oxidation is so slight that it can hardly be observed in the XRD pattern shown in Fig. 1(b).

To protect the $Mg_2Si_{0.4}Sn_{0.6}$ pellets from oxidation in air as well as in inert gases, we applied an Al_2O_3 thin-film coating on the $Mg_2Si_{0.4}Sn_{0.6}$ surface, expecting the dense Al_2O_3 layer would effectively protect the sample from contacting oxygen and corrosive vapors. To study the oxidation resistance of the Al_2O_3 thin-film coating, TGA analysis was also conducted on the

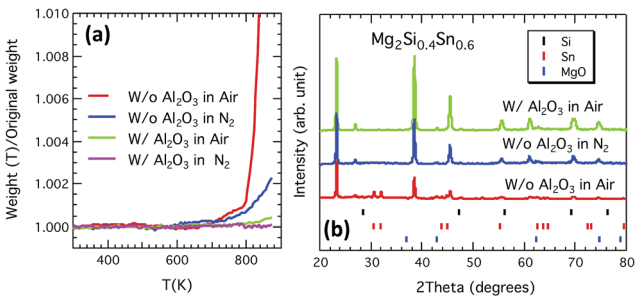

Fig. 1 (a) Thermogravimetric analysis of the as-made $Mg_2Si_{0.4}Sn_{0.6}$ pellets in flowing air (red curve) and in flowing N_2 (blue curve); thermogravimetric analysis of the Al_2O_3-coated $Mg_2Si_{0.4}Sn_{0.6}$ pellets in flowing air (green curve) and in flowing N_2 (pink curve); (b) the XRD profiles of the $Mg_2Si_{0.4}Sn_{0.6}$ pellets after TGA measurement. The XRD peak positions of Si, Sn, and MgO phases are denoted by the vertical sticks.

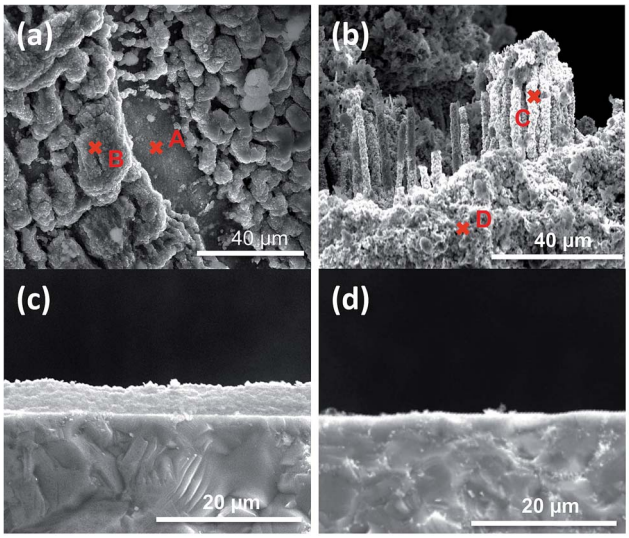

Fig. 2 SEM images of (a) surface and (b) cracked cross-section of the as-made $Mg_2Si_{0.4}Sn_{0.6}$ pellet after TGA measurement in flowing air, (c) cross-section of the as-made $Mg_2Si_{0.4}Sn_{0.6}$ pellet measured in flowing N_2, and (d) cross-section of the Al_2O_3-coated $Mg_2Si_{0.4}Sn_{0.6}$ pellet measured in flowing air.

Al_2O_3-coated $Mg_2Si_{0.4}Sn_{0.6}$ pellets in air and N_2. As shown in Fig. 1(a), the Al_2O_3-coated sample measured in air gained very little weight above 800 K; the same Al_2O_3-coated sample heated in N_2 was stable up to 873 K.

The $Mg_2Si_{0.4}Sn_{0.6}$ samples after TGA analysis were examined with SEM to investigate the morphology change. After heating in air, the as-made $Mg_2Si_{0.4}Sn_{0.6}$ pellet became brittle and cracked; we examined both the surface and the cracked cross-section of the sample as is shown in Fig. 2(a) and (b), respectively. Fig. 2(a) shows that on the surface of the as-made $Mg_2Si_{0.4}Sn_{0.6}$ pellet heat-treated in air, there exist flat terrains (denoted by letter A) surrounded by raised and porous structures (denoted by letter B). We analyze the atomic ratios of Mg, Si, and Sn within these two areas using EDX. The EDX results listed in Table 1 indicate that the flat terrain is Si-rich while the raised porous structure is Sn-rich. Yin *et al.* have reported that $Mg_2Si_{1-x}Sn_x$ solid solutions decompose into Sn-rich and Si-rich phases during heat treatment due to a peritectic reaction.[10] Fig. 2(a) suggests that the degradation in the Sn-rich phase is more severe than in the Si-rich phase, which is consistent with Skomedal *et al.*'s conclusion that the Sn-rich phase can be oxidized at a faster rate and at lower temperatures.[9] In Fig. 2(b), we found that inside the collapsed sample, there are micron-sized free-standing pillars (denoted by letter C). EDX analysis indicates that the pillars are significantly Sn-rich while the porous bulk beneath the pillars (denoted by letter D) is Si-rich. As shown in Table 1, the Mg atomic ratio in the bulk (region C and D) is significantly lower than that on the surface (region A and B). These results suggest that during heat treatment, Mg in the bulk tends to migrate to the surface and react with oxygen, which results in a Mg-deficient bulk. Moreover, since the Mg concentration is higher in the Sn-rich pillars (C) than in the Si-rich bulk (D), the Sn-rich phase appears to be liquefied at high temperatures, to further facilitate Mg migration from the bulk to the surface. However, further investigation may be conducted in order to understand fully the decomposition mechanism of $Mg_2Si_{1-x}Sn_x$ solid solutions.

Table 1 The atomic ratios of Mg, Si and Sn in different locations marked by the symbol "×" in Fig. 2(a) and (b) analyzed by energy-dispersive X-ray spectroscopy

Atomic ratio	Mg%	Si%	Sn%
$Mg_2Si_{0.4}Sn_{0.6}$	66.7	13.3	20.0
A	89.0	7.1	3.9
B	85.7	0.4	13.8
C	51.9	0.7	47.4
D	41.9	43.7	14.4

As shown in Fig. 2(c), the as-made $Mg_2Si_{0.4}Sn_{0.6}$ sample was uniformly covered with a porous layer of MgO after heat treatment in N_2. In contrast, Fig. 2(d) show a clear surface of the Al_2O_3-coated sample after heat treatment in air. Although these two samples show little difference in their XRD patterns in Fig. 1(b), both the TGA and SEM analysis suggest that the uncoated $Mg_2Si_{0.4}Sn_{0.6}$ sample is more vulnerable to oxidation even though the heating is conducted in N_2.

To study further the thermal stability of $Mg_2Si_{0.4}Sn_{0.6}$ at elevated temperatures for extended hours, we annealed two $Mg_2Si_{0.4}Sn_{0.6}$ pellets, with and without Al_2O_3 coating, in a tube furnace where the argon gas (ultra high purity, 99.999%) was flowing through. Fig. 3(a) shows the two pellets before annealing. Although the Al_2O_3 coating is only 18 nm thick, it changes the pellet color from metallic silver to purple red due to thin film interference. After being annealed at 823 K for 12 hours in flowing argon, the as-made pellet was totally decomposed, as shown in Fig. 3(b). The XRD profile shown in Fig. 3(c) indicates the as-made $Mg_2Si_{0.4}Sn_{0.6}$ pellet completely decomposed into MgO, Si and Sn:

$$Mg_2Si_{0.4}Sn_{0.6} + O_2 = 2MgO + 0.4Si + 0.6Sn \quad (2)$$

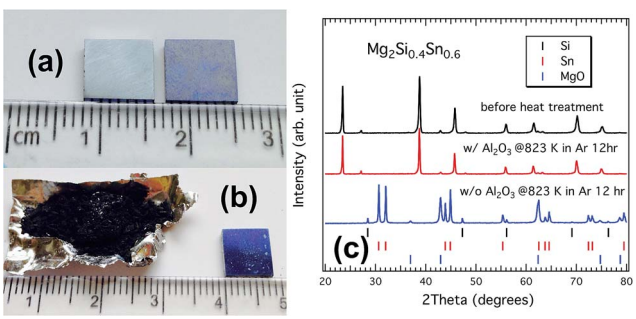

Fig. 3 (a) Image of $Mg_2Si_{0.4}Sn_{0.6}$ pellets with (right) and without (left) Al_2O_3 thin-film coating. (b) Image of the pellets described in (a) after being annealed at 823 K for 12 hours in flowing argon; the bare pellet totally decomposed into a powder that was collected on a platinum foil. (c) The XRD patterns for the sample before annealing (black curve), the Al_2O_3-coated sample after annealing (red curve), and the as-made pellet after annealing (blue curve). The as-made sample after annealing consists of Si, Sn, and MgO phases, whose XRD peak positions are indicated by the vertical sticks.

Table 2 Brief summary of protective coatings of $Mg_2Si_xSn_{1-x}$ compounds

Coating/bulk material	Coating technique	Thickness	Maximum working temperature (K)	Testing duration (h)
β-$FeSi_2$/Mg_2Si (ref. 6)	RF magnetron sputtering	0.7 μm	873	3
Al_2O_3/$Mg_2Si_{0.4}Sn_{0.6}$ (ref. 9)	N/A	20 μm	623	24
BN/$Mg_2Si_{0.3}Sn_{0.7}$ (ref. 10)	Spray	0.5 mm	773	720
Al_2O_3/$Mg_2Si_{0.4}Sn_{0.6}$ [this work]	ALD	18 nm	823	12

Bourgeois *et al.*'s study has suggested that a $Mg_2Si_{1-x}Sn_x$ pellet could be partially oxidized under inert gas atmosphere.[7] However, our study further suggested that when the $Mg_2Si_{0.4}Sn_{0.6}$ is exposed to the low level of residual oxygen in inert gas for extended hours, the solid solution phase would completely decompose. On the other hand, the Al_2O_3-coating again exhibits an effective oxidation-resistance as under the same heat treatment, the Al_2O_3-coated pellet shows no change in appearance as well as in the XRD pattern. Table 2 lists the details of our ALD-deposited Al_2O_3 coating in comparison to other protective coatings reported previously.[6,9,10] One key advantage of this nano-scale Al_2O_3 coating is that it can provide *in situ* protection of $Mg_2Si_{0.4}Sn_{0.6}$ during high-temperature measurements, which will be discussed in Section III C.

B. Thermoelectric properties

Thermoelectric-property measurements of $Mg_2Si_{1-x}Sn_x$ were mostly conducted in inert gas atmospheres. In Section III A, however, we have demonstrated that even in inert gas atmosphere, unprotected $Mg_2Si_{1-x}Sn_x$ pellets suffer oxidation to some extent depending on the residual oxygen level. In this section, we attempt to investigate whether a slight oxidation would alter the thermoelectric properties of $Mg_2Si_{0.4}Sn_{0.6}$. In order to achieve the optimal *ZT* by fine tuning the carrier concentration, $Mg_2Si_{0.4}Sn_{0.6}$ is usually doped with Sb at the concentration of 0.5–1.5 atm%. The following $Mg_2Si_{0.4}Sn_{0.6}$ samples were doped with 0.5 or 1.5 atm% Sb. It is believed that Sb doping at this concentration would not affect the thermal stability of $Mg_2Si_{.0.4}Sn_{0.6}$.

Two rectangular-shaped $Mg_2(Si_{0.4}Sn_{0.6})_{0.985}Sb_{0.015}$ samples, with and without Al_2O_3 thin-film coating, were heated in an Ar-flowing tube furnace with the temperature ramping to 823 K at the rate of 3 K min^{-1} and then cooled down naturally without dwelling. The uncoated sample after the temperature cycle was covered with a layer of white MgO powder and the Al_2O_3-coated sample had no visible change. After removing the surface layer, however, the XRD patterns show no distinct difference between these two samples. We then conducted thermoelectric-property measurements on these two samples from 2 K to 400 K by using the thermal transport option in PPMS. As shown in Fig. 4(a), the heat treatment did not change the figure-of-merit (*ZT*) of the Al_2O_3-coated sample, but it significantly reduced the *ZT* of the unprotected $Mg_2Si_{0.4}Sn_{0.6}$ sample by 28% at 300 K. When looking further into the thermoelectric properties shown in Fig. 4(b–d), it is clear that the decrease of *ZT* in the unprotected $Mg_2Si_{0.4}Sn_{0.6}$ sample is due to a reduction of carrier concentration during the heat treatment. A calculation based on the

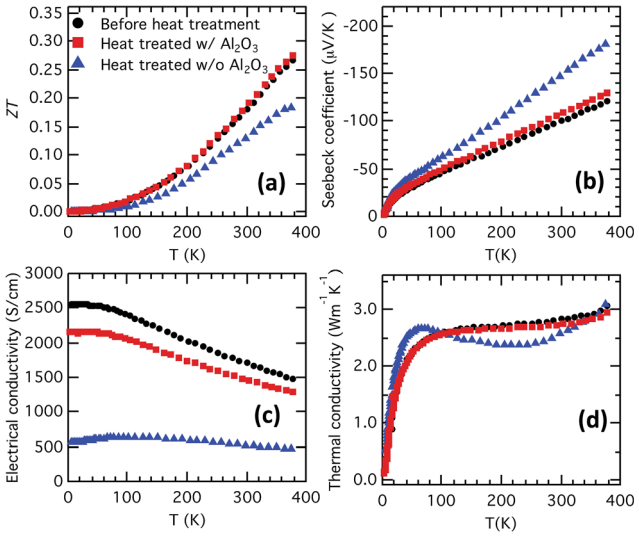

Fig. 4 Temperature dependences of (a) dimensionless figure-of-merit (*ZT*), (b) Seebeck coefficient, (c) electrical conductivity and (d) thermal conductivity of the $Mg_2(Si_{0.4}Sn_{0.6})_{0.985}Sb_{0.015}$ sample before a temperature cycle (denoted with black dot), Al_2O_3-coated $Mg_2(Si_{0.4}Sn_{0.6})_{0.985}Sb_{0.015}$ sample after a temperature cycle (red square), and the as-made $Mg_2(Si_{0.4}Sn_{0.6})_{0.985}Sb_{0.015}$ sample after a temperature cycle (blue triangle).

room temperature Seebeck coefficient shows that the carrier concentration in the as-made sample dropped from 2.5×10^{20} cm^{-3} before heat treatment to 0.7×10^{20} cm^{-3} after heat treatment. This significantly reduced carrier concentration leads to the higher value of Seebeck coefficient, the much-reduced electrical conductivity, the decreased electronic thermal conductivity, and a lower *ZT*.

In order to confirm that the changes in thermoelectric properties are caused by oxidation instead of the inhomogeneity of the original sample, we conducted a scanning Seebeck coefficient measurement on a 6 mm × 6 mm × 1 mm $Mg_2(Si_0Sn_{0.6})_{0.995}Sb_{0.005}$ sample. One half of the pellet was coated with Al_2O_3 while the other half was uncoated. The square pellet then was subjected to a temperature cycle from room temperature to 823 K in an Ar-flowing tube furnace. Afterwards, the pellet surface was polished for scanning Seebeck coefficient measurement. As shown in Fig. 5, the Seebeck coefficient on the left side is more homogeneous and the average value is around −130 μV K^{-1}. In contrast, the average value of the Seebeck coefficient on the right side of the pellet is clearly higher, suggesting that oxidation is the major cause of the reduced carrier concentration.

This observation indicates that the decrease of carrier concentration is associated with the Mg vacancies created in $Mg_2Si_{0.4}Sn_{0.6}$ lattice during oxidation:

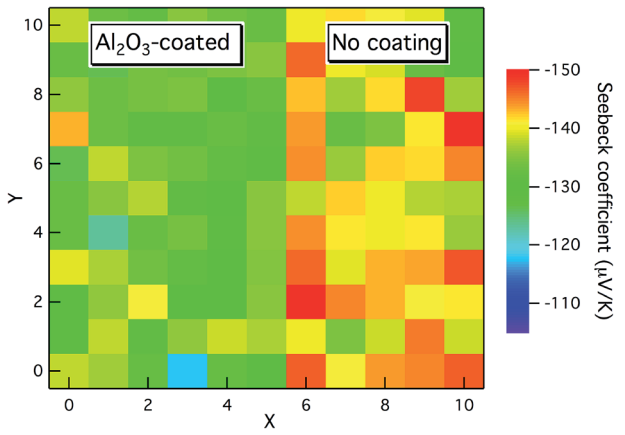

Fig. 5 Scanning Seebeck coefficient measurement on a 6 mm × 6 mm × 1 mm $Mg_2(Si_{0.4}Sn_{0.6})_{0.995}Sb_{0.015}$ square pellet after thermal treatment; a total of 11 × 11 data points were collected across the sample. Before heat treatment, the left side of the sample was coated with an Al_2O_3 thin film; the right side of the sample had no coating. After heat treatment, the whole sample surface was polished for scanning Seebeck coefficient measurement.

$$Mg_2Si_{0.4}Sn_{0.6} + \delta O_2 = Mg_{2-2\delta}Si_{0.4}Sn_{0.6} + 2\delta MgO \quad (3)$$

In our previous study, we proposed that Mg vacancies in the $Mg_2Si_{0.4}Sn_{0.6}$ lattice can form localized hole states, which trap the Sb-dopant electrons and thus reduce the carrier concentration.[15] This localized Mg-vacancy states model was supported by experimental and calculation results.[15] Yin *et al.* have also reported a decrease in carrier concentration that is associated with Mg loss in the $Mg_2Si_{0.3}Sn_{0.7}$ matrix. They also observed a reduced *ZT* in $Mg_2Si_{0.3}Sn_{0.7}$ after the sample was annealed in air at 823 K.[10] On the other hand, Bourgeois *et al.* found in the undoped $Mg_2Si_{1-x}Sn_x$ compound, the transport properties are repeatable under thermal cycles even through the phase does not seem stable.[7] As mentioned in Section I, these two observations do not contradict with each other. In Bourgeois' study, the undoped $Mg_2Si_{1-x}Sn_x$ solid solutions were intrinsic semiconductors. After Mg vacancies are created during thermal cycles, they form localized in-gap states instead of contributing free holes.[15] Therefore, the presence of Mg vacancies in intrinsic $Mg_2Si_{1-x}Sn_x$ do not change the carrier concentration significantly. In both works from Yin *et al.* and the present study, the $Mg_2Si_{1-x}Sn_x$ compound is doped with Sb. The in-gap states induced by Mg vacancies can trap the Sb dopant electrons and significantly reduce the carrier concentration. In practical thermoelectric applications, $Mg_2Si_{1-x}Sn_x$ solid solutions are usually doped with an adequate amount of Sb or Bi in order to achieve an optimal carrier concentration. Therefore, if the material suffers Mg loss under heat treatment, the carrier concentration and electrical conductivity would deteriorate.

C. Laser-flash measurements

The laser-flash method is commonly employed to measure the thermal diffusivities, which enables the calculation of thermal conductivities above room temperature.[16] In this section, we demonstrate that sample oxidation introduces errors in the laser flash measurement. Fig. 6 shows the thermal diffusivity results of Sb-doped $Mg_2Si_{0.4}Sn_{0.6}$ samples measured by the laser-flash method. The thermal diffusivity curves of the unprotected samples do not overlap on heating up and cooling down, even though the measurement is carried out in flowing helium gas (ultra high purity, 99.999%). In one measurement cycle, the thermal diffusivity results measured during heating up are generally higher than those measured during cooling down. We believe that this deviation of thermal diffusivity results is caused by the Mg oxidation on the samples surface, which not only reduces carrier concentration, but also separates the graphite coating layer from the sample surface during the measurement. In a standard laser-flash measurement, a thin graphite coating is required on both sides of a sample to absorb the laser heat at the front side and to assist the emission at the rear side. For $Mg_2Si_{1-x}Sn_x$ samples, however, we observed that the graphite layer was exfoliated from the sample surface after measurement. A MgO layer appears to grow on the $Mg_2Si_{1-x}Sn_x$ surface during the measurement and prevents the graphite layer from adhering to the sample surface. The exfoliation of the graphite layer during measurement largely offsets the laser pulse absorption and gives rise to notably smaller thermal diffusivity values.

In order to solve the sample oxidation and graphite-exfoliation problem, we applied the Al_2O_3 thin-film coating to provide an *in situ* protection to the $Mg_2Si_{1-x}Sn_x$ pellet during the laser-flash measurement. Fig. 6 shows that the thermal diffusivity results of the Al_2O_3-coated sample are consistent and independent of the temperature ramping directions. One may be curious whether the Al_2O_3 coating alters the sample's thermal diffusivity results. In order to address this concern, we have compared two fresh samples, one with the coating and the other without the coating and found their thermal diffusivities are identical at room temperature. Therefore, the Al_2O_3 thin-film coating is proven to be a good strategy to avoid measurement errors in the laser-flash measurements for $Mg_2Si_{1-x}Sn_x$ solid solutions.

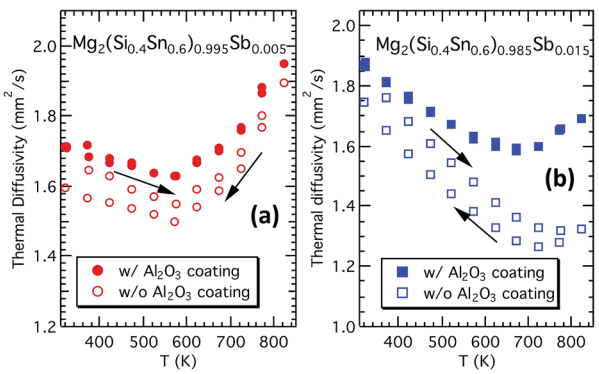

Fig. 6 Temperature dependence of thermal diffusivity of (a) $Mg_2(Si_{0.4}Sn_{0.6})_{0.995}Sb_{0.005}$ and (b) $Mg_2(Si_{0.4}Sn_{0.6})_{0.985}Sb_{0.015}$ measured by the laser-flash method. The filled symbols denote the samples coated with Al_2O_3 thin film during measurement; the hollow symbols denote the samples without the Al_2O_3 coating during measurement.

IV. Conclusions

In this work, we found that $Mg_2Si_{0.4}Sn_{0.6}$ solid solution is not stable at high temperatures even under an inert-gas atmosphere. At temperatures above 700 K, the Mg element in this material becomes oxidized by residual oxygen in the inert gas; however, the oxidation is not as vigorous as in air. The Mg oxidation in $Mg_2Si_{0.4}Sn_{0.6}$ leads to phase decomposition into Si-rich and Sn-rich phases. Our results indicate that the Sn-rich phase melts as temperature increases, which accelerates the Mg migration from the bulk into the surface and the Mg oxidation. We also demonstrated that the oxidation of Sb-doped $Mg_2Si_{0.4}Sn_{0.6}$ in the inert gas reduces the carrier concentration and deteriorates the figure-of-merit of the material.

To protect the material from thermal degradation, we applied a nanoscale Al_2O_3 thin-film coating on the sample's surface to prevent the sample from exposure to residual oxygen. The Al_2O_3-coated $Mg_2Si_{0.4}Sn_{0.6}$ exhibited a good oxidation resistance at 823 K for 12 hours and stable thermoelectric properties upon temperature cycling in Ar gas. Last but not least, we revealed that the inconsistency in thermal diffusivity results in $Mg_2Si_{1-x}Sn_x$ is caused by sample oxidation and associated graphite exfoliation during the laser-flash measurement. It has been demonstrated that the $Mg_2Si_{0.4}Sn_{0.6}$ samples with the nanoscale Al_2O_3 coating can give rise to consistent thermal diffusivity results in the laser-flash measurement.

Acknowledgements

This work was supported by the National Science Foundation (NSF)-Department of Energy (DOE) Joint Thermoelectric Partnership (NSF Award No. CBET1048767). The SPS equipment used for materials consolidation was acquired with the support of a NSF Major Research Instrumentation (MRI) award (DMR-1229131). The PPMS instrument for thermoelectric measurements was acquired with the support of the NSF Materials Interdisciplinary Research Team (MIRT) award (DMR1122603). The scanning Seebeck measurements were acquired with the support of Solid-State Solar-Thermal Energy Conversion Center (S3TEC), an Energy Frontier Research Center funded by the U.S. Department of Energy, Office of Science, Basic Energy Sciences under Award No. DE-SC0001299.

References

1 D. M. Rowe, *Thermoelectrics handbook: macro to nano*, CRC press, 2005.
2 V. Zaitsev, M. Fedorov, I. Eremin and E. Gurieva, *Thermoelectrics handbook: macro to nano*, CRC Press, 2005, ch. 29.
3 V. Zaitsev, M. Fedorov, E. Gurieva, I. Eremin, P. Konstantinov, A. Y. Samunin and M. Vedernikov, *Phys. Rev. B: Condens. Matter Mater. Phys.*, 2006, **74**, 045207.
4 W. Liu, X. Tan, K. Yin, H. Liu, X. Tang, J. Shi, Q. Zhang and C. Uher, *Phys. Rev. Lett.*, 2012, **108**, 166601.
5 Q. Zhang, J. He, T. Zhu, S. Zhang, X. Zhao and T. Tritt, *Appl. Phys. Lett.*, 2008, **93**, 102109.
6 J.-i. Tani, M. Takahashi and H. Kido, *J. Alloys Compd.*, 2009, **488**, 346.
7 J. Bourgeois, J. Tobola, B. Wiendlocha, L. Chaput, P. Zwolenski, D. Berthebaud, F. Gascoin, Q. Recour and H. Scherrer, *Funct. Mater. Lett.*, 2013, **6**, 1340005.
8 M. Søndergaard, M. Christensen, K. A. Borup, H. Yin and B. B. Iversen, *J. Mater. Sci.*, 2013, **48**, 2002.
9 G. Skomedal, N. R. Kristiansen, M. Engvoll and H. Middleton, *J. Electron. Mater.*, 2014, **43**, 1946.
10 K. Yin, Q. Zhang, Y. Zheng, X. Su, X. Tang and C. Uher, *J. Mater. Chem. C*, 2015, **3**, 10381.
11 B. Hoex, J. Schmidt, P. Pohl, M. Van de Sanden and W. Kessels, *J. Appl. Phys.*, 2008, **104**, 044903.
12 G. Dingemans and W. Kessels, *J. Vac. Sci. Technol., A*, 2012, **30**, 040802.
13 L. Zhang, P. Xiao, L. Shi, G. Henkelman, J. B. Goodenough and J. Zhou, *J. Appl. Phys.*, 2015, **117**, 155103.
14 G. J. Snyder, Scanning measurement of Seebeck coefficient of a heated sample, *US Pat.*, App. 13/547, 006, 2012.
15 L. Zhang, P. Xiao, L. Shi, G. Henkelman, J. B. Goodenough and J. Zhou, *J. Appl. Phys.*, 2016, **119**, 085104.
16 W. Parker, R. Jenkins, C. Butler and G. Abbott, *J. Appl. Phys.*, 1961, **32**, 1679.